Exhaled Breath Sensors

Il-Doo Kim, Seon-Jin Choi, Sang-Joon Kim and Ji-Su Jang

Abstract This chapter reports a comprehensive review of the state-of-the-art in research on daily health monitoring and early diagnosis of specific diseases via the analysis of exhaled breath biomarkers. Different types of breath analyzing techniques including gas chromatography/mass spectroscopy (GC/MS), selected-ion flow-tube mass spectroscopy (SIFT-MS), and proton transfer reaction-mass spectrometry (PTR-MS) are compared to evaluate the unique strengths of each method. Recently, as an emerging breathsensing technique, we highlight chemiresistive-type gas sensors with characteristics of portability, cost effectiveness, and real-time analysis. Among various diseases, we focused on studies related to the diagnosis of diabetes and lung cancer. A number of studies have demonstrated a strong correlation between exhaled breath components and specific diseases, thus offering strong potential for clinical diagnostic application using exhaled breath sensors. In addition, we also summarized recent progress on daily healthcare such as fat-burning and halitosis through breath analysis. Finally, future perspectives on clinical applications using breath analyzing techniques are discussed.

Keywords Breath analysis · Sensor · Diabetes · Lung cancer · Halitosis · Fat burning

1 Introduction

1.1 Disease Markers in Exhaled Breath Gases

Human breath contains a number of volatile organic compounds (VOCs). Accurate detection of specific VOCs in exhaled breath, known as biomarkers, can provide essential information for the diagnosis of specific diseases. Breath analysis is a very

I.-D. Kim (✉) · S.-J. Choi · S.-J. Kim · J.-S. Jang
Department of Materials Science and Engineering, Korea Advanced Institute of Science and Technology, 291 Daehak-ro, Yuseong-gu, Daejeon 305-701, People's Republic of Korea
e-mail: idkim@kaist.ac.kr

C.-M. Kyung (ed.), *Smart Sensors for Health and Environment Monitoring*,
KAIST Research Series, DOI 10.1007/978-94-017-9981-2_2

powerful tool for clinical diagnostics because it is noninvasive, painless, cost effective, and easily repeated [1–4]. The variations in the concentration of the exhaled VOCs that may serve as biomarkers for specific diseases can be used as clinical information for distinguishing healthy and sick people. A number of biomarkers in exhaled breath, which have strong correlations with specific diseases, have been identified in various studies [5–8]. For example, hydrogen sulfide, acetone, toluene, ammonia, nitrogen monoxide, and pentane are known to have strong relationships with halitosis, diabetes, lung cancer, kidney failure, asthma, and heart disease, respectively. In particular, nitrogen monoxide sensors for the monitoring of asthma have been successfully commercialized [9, 10]. Moreover, intensive research is still underway to develop breath analyzing devices with high accuracy for early detection of lung cancer and diabetes. Recently, new attempts related to daily health monitoring such as halitosis and fat burning using analysis of exhaled breath have been introduced. In this chapter, several types of exhaled breath sensors as well as recently identified pathological exhaled biomarkers with respect to specific diseases will be presented.

1.2 Various Tools for Analysis of Exhaled Breath Gases

The noninvasive diagnosis for various diseases is a distinctive advantage of exhaled breath analysis techniques as compared to commonly used methods (e.g., computed tomography or an endoscope) which are often invasive and complex. For this reason, gas detection techniques such as gas chromatography/mass spectroscopy (GC/MS), [11, 12] selected-ion flow-tube mass spectroscopy (SIFT-MS), proton transfer reaction-mass spectrometry (PTR-MS), and semiconductor metal oxide (SMO)-based chemiresistive sensors have been widely adopted to detect sub-ppm concentrations of VOCs in exhaled breath. Highly sensitive and selective detection of exhaled breath components has been achieved using these techniques for clinical diagnostic application. The basic operating principles as well as strengths and weaknesses of each method are summarized in Table 1. GC-MS is a commonly used analysis technique to identify traces of VOCs in exhaled breath. To separate the VOC compounds, two types of chromatographic columns, i.e., polar and nonpolar columns, are generally used [13]. A nonpolar column can separate VOC components according to the boiling points. On the other hand, a polar column separates VOC compounds depending on the polarity difference. The separated compounds are analyzed by MS for quantification of the individual compounds in breath. A statistical analysis of the data obtained by GC-MS measurement is then accompanied to identify the disease biomarkers. Although GC-MS shows high sensitivity of ppb level in the analysis of breath components, a time-consuming process accompanying preconcentration steps limits its practical application. For this reason, real-time analysis techniques such as PTR-MS and SIFT-MS are widely used [14–17]. PTR-MS measures the ionized VOCs produced by reaction with

Table 1 Comparison of breath analysis techniques

Types	Principle	Merit	Demerit
GC-MS	Analyzing separated compounds by MS using chromatographic column (polar or non-polar)	Capability of ppb detection	Preconcentration steps, bulky, expensive, and requires trained operator
PTR-MS	Analyzing ionized molecules of target analytes by reaction with H_3O^+ by MS	Real-time, capability of ppt detection	Lack of specificity, bulky, and requires trained operator
SIFT-MS	Analyzing ions produced by the reaction of analytes and precursor ions (H_3O^+, NO^+ or O_2^+) by quadrupole MS	Real-time, capability of ppt detection	Bulky, and requires trained operator
SMO-based chemiresistive-type sensor	Measuring resistivity changes based on the thinning or thickening the depletion layer of n-type SMOs and hole accumulation layer of p-type SMOs around the surface when exposed to oxidizing or reducing gas ambient	Real-time, portable, inexpensive, and capability of sub-ppm detection	Relatively low sensitivity and less selectivity

precursor hydronium ions (H_3O^+) in a drift-tube reactor. PTR-MS with high sensitivity, which can detect ppt levels of VOCs in breath within 10 s, allows online breath analysis. However, it is difficult to specify a number of VOCs using only PTR-MS due to limited numbers of precursors.

The lack of specificity of PTR-MS can be addressed by SIFT-MS. SIFT-MS utilizes three ion precursors, i.e., H_3O^+, NO^+, and O_2^+, for chemical ionization in a flow tube with VOCs, in contrast with PTR-MS, which uses only one ion precursor of H_3O^+. The ion precursors of NO^+ and O_2^+ are capable of identifying VOC compounds such as light hydrocarbons and halogenated species, which do not react with H_3O^+. SIFT-MS can thus very sensitively detect ppt levels of VOCs with a real-time quantitative analysis, allowing online breath identification. However, analyzing equipment such as GC-MS, PTR-MS, and SIFT-MS are bulky and expensive, which limits application for portable devices. An emerging chemiresistive-type breathsensing technique using SMO-based materials is receiving attention due to its high potential for miniaturization to develop portable diagnostic devices. A simple analyzing principle by measuring resistivity changes of SMO-based materials is advantageous for low cost analysis techniques. A resistivity change occurs by thinning or thickening the depletion layer of n-type SMOs and hole accumulation layer of p-type SMOs around the surface. For example, n-type SMOs such as SnO_2 (tin oxide), WO_3 (tungsten oxide), and ZnO

(zinc oxide) enter a high resistivity state when exposed to ambient air by thickening the surface depletion layers. This is attributed to electron attraction from the conduction band of SMOs by chemically adsorbed oxygen species such as O^-, O_2^-, and O^{2-}. When reducing VOCs such as hydrogen sulfide, acetone, and toluene are exposed to n-type SMOs, the adsorbed oxygen species are eliminated by donating the bound electrons to conduction band, thereby thinning the depletion layer, which results in decreased resistivity. The fast responding resistivity changes depending on the measurement ambient allow real-time diagnosis of disease by a breath analysis. However, low sensitivity and less selectivity of SMO-based sensors are limitations for precise diagnosis of diseases. For this reason, highly sensitive as well as extremely selective VOC sensing SMO layers, i.e., materials and structures, should be developed [18].

The current analysis techniques have several advantages and disadvantages. Therefore, adequate breath analysis techniques should be selected depending on the concentration ranges of the targeted biomarkers.

2 Exhaled Breath Sensors for Diagnostic Application

2.1 Halitosis

Halitosis, commonly called bad breath or oral malodor, is a symptom where a markedly unpleasant odor presents in the exhaled breath. It is a very offensive symptom that has adverse social and quality of life implications. Halitosis can be categorized into two types, i.e., intra-oral halitosis and extra-oral halitosis [19]. Intra-oral halitosis originating from the mouth is mainly caused by gum disease, dental caries, bacterial imbalance on the tongue, impacted wisdom teeth, and dehydration. In the case of extra-oral halitosis, it can occur by digestive tract conditions such as gastroesophageal reflux disease (GERD), stomach and duodenal ulcers, and disorders in organs such as the liver and kidneys [20]. Intra-oral halitosis patients account for 90 % of the total halitosis patients, whereas the remaining 10 % are extra-oral halitosis patients [19]. Among the two types of halitosis, extra-oral halitosis is particularly important for diagnosis and cure, considering that it is related to organ malfunctions. To provide adequate medical treatment, it is important to identify the cause of the malodor. Basically, a malodor is composed of volatile sulfur compounds (VSCs) such as hydrogen sulfide (H_2S), methyl mercaptan (CH_3SH), and dimethyl sulfide (CH_3SCH_3), whose concentrations exceed 1 ppm for halitosis patients, whereas their concentrations are less than 150 ppb for healthy people [21]. H_2S and CH_3SH are the dominant species accounting for 90 % of the total VSCs in the breath to determine the degree of halitosis [22]. In the case of intra-oral halitosis, the basic mechanism of VSC generation in exhaled breath of halitosis patients is based on the breakdown of proteins, i.e., cysteine, methionine, tryptophan, and lysine, [23] into individual amino acids, followed by further

breakdown of certain amino acids to produce H_2S and CH_3SH. In addition, tongue bacteria located on the coating tongue, microbial putrefaction of food debris, cells, and saliva also produce VSCs [24]. On the other hand, extra-oral halitosis can occur by metabolic disorders. Specifically, odiferous agents such as VSCs circulating in the bloodstream can be exhaled, through alveolar gas exchange, into the breath and cause malodor [23].

To diagnose and treat the halitosis, various methods of detecting malodor have been proposed, including an organoleptic test, [22] and a benzoyl-DL-arginine-naphthylamide (BANA) test, [25] based on measurement of salivary levels of an enzyme indicating the presence of certain halitosis-related bacteria. Among the current diagnostic methods, it is a notable advantage that halitosis can be easily identified by analyzing the VSCs concentration in exhaled breath. For this reason, exhaled breath analysis for diagnosis of halitosis has been intensively studied using GC-MS, which shows highly sensitive detection capability at ppb levels [26]. As clinical diagnostic techniques, exhaled breath analysis is typically accomplished using a breath analyzer such as Halimeter® (Interscane Co., USA), [27] Breathtron™ (New Cosmos Electric Co., Ltd, Japan), [28] and OralChroma™ (Abilit Co., Japan), [29] which are specialized for the detection of VSCs. Table 2 summarizes the three types of breath analyzers for diagnosis of halitosis by detection of VSCs. As shown in Table 2, Halimeter®, which is operated by an electrochemical voltammetric technique, shows a detection limit of 5 ppb with relatively short measurement time (approximately 1 s). In the case of Breathtron™, a metal oxide-type sensor capable of detection as low as 10 ppb and rapid sensing of 45 s is utilized. In addition, GC type of OralChroma™ showed very sensitive detection of 1 ppb, but relatively long measurement time ($\sim$480 s).

Tsai et al. performed in-depth studies of intra-oral halitosis for the detection of VSCs in exhaled breath. The experiment was performed with GC-type OralChroma™ and an organoleptic test for analysis of the correlation between concentrations of VSCs and oral hygiene status [22]. The experiment on each patient (42 men, 30 women, 19–64 years, mean age 46.83 ± 10.18 years) was carried out with four continuous steps, i.e., baseline step (before removing tongue coating), tongue scraping step (after removing tongue coating), nonsurgical periodontal therapy step, and oral hygiene instruction/chlorhexidiene-2 or chlorhexdiene-4 step. Figure 1a shows the trend of the organoleptic test scores

Table 2 Three types of breath analyzers for halitosis diagnosis by detection of VSCs

Equipment	Sensor principle of operation	Detection limit (ppb)	Testing ambient (% RH)	Lag time (s)	Dimensions/weight	Ref.
Halimeter®	Electrochemical voltammetric	5	95	<1	114 × 254 × 267 mm/3.6 kg	[27]
Breathtron™	Metal oxide sensor	10	95	45	150 × 230 × 150 mm/2 kg	[28]
OralChroma™	Gas chromatographs	1	80	480	280 × 130 × 400 mm/5.5 kg	[29]

(0, no odor; 1, noticeable odor; 2, clearly noticeable odor; 3, moderate odor; 4, strong odor; 5, extremely foul odor) and tongue-coating scores at different experiment stages. The results indicated that the degree of tongue coating has a strong correlation with the organoleptic score exhibiting proportional relation (Fig. 1a). In addition, the concentrations of H_2S and CH_3SH significantly decrease gradually after removing the tongue coating or undergoing oral treatment (Fig. 1b). This means that, eventually, the periodontal treatment or removing tongue coating can effectively prevent halitosis, identified both in the organoleptic test score and in the objective measurement of VSCs.

Although the GC analyzing method is highly sensitive and selective for diagnosis of halitosis, it is expensive, involves a complex analysis, and is inconvenient for portable use. In particular, the issue of portability is particularly important considering that halitosis should be diagnosed in real-time for daily healthcare purposes. For this reason, a portable diagnostic device with real-time monitoring as well as outstanding VSC sensitivity should be developed. In this regard, chemiresistive-type SMOs are promising sensing layers for diagnosis of halitosis through portable and real-time diagnostic applications because of their facile operating principle (resistivity change upon exposure of VSCs to the SMO's surface layers), simple device fabrication, and ready miniaturization [30]. Table 3 summarizes recent publications for halitosis diagnosis by detection of H_2S using SMO-based sensing layers. As shown in Table 3, most chemiresistive SMO sensors exhibited faster responding time (1–300 s) in comparison with a GC-MS analyzer (480 s) and highly sensitivity for H_2S detection (approximately 1 ppb to 1 ppm). Recently, nanostructured SMOs using various materials have been reported for improving sensing performance such as sensitivity, selectivity, and response speed. In addition, different types of catalysts, i.e., noble metallic catalysts such as Pt, [31] and Au, [32] metal oxide catalysts such as CuO, [33] MoO_3, [34] and IrO_2, [35] and graphene-based catalytic materials such as graphite, graphene oxide, and reduced graphene oxide, are functionalized with SMOs for improved selectivity and sensitivity toward H_2S molecules. For example, Shin et al. [35] synthesized WO_3 nanofibers functionalized by catalytic Pt nanoparticles and demonstrated their superior H_2S sensing characteristics, thereby illustrating their capability for application in halitosis diagnosis.

Furthermore, exhaled breath sensors with hollow SMOs structures functionalized by uniformly distributed noble metallic nanoparticles exhibiting an average size of 6.45 nm were proposed for the diagnosis of halitosis. Choi et al. [32] presented a simple synthetic method for loading Au nanoparticles on the inner shell of hollow SnO_2 hemispheres using a sacrificial template of Au decorated block copolymer (Au-BCP) spheres. The block copolymer spheres were synthesized by an oil–water emulsion of polystyrene-*b*-poly (4-vinylpyridine) (PS-*b*-P4VP) block copolymers (Fig. 2a). Au precursors infiltrated the prepared block copolymer spheres under an acidic condition to produce Au-BCP (Fig. 2b) [40, 41]. The SnO_2 layer was then deposited on the Au-BCP spheres using RF magnetron sputtering. The deposition proceeded for 210 s to coat a SnO_2 film on Au-BCP spheres with 20 nm-thick shells. After coating the SnO_2 layer on Au-BCP spheres, the samples

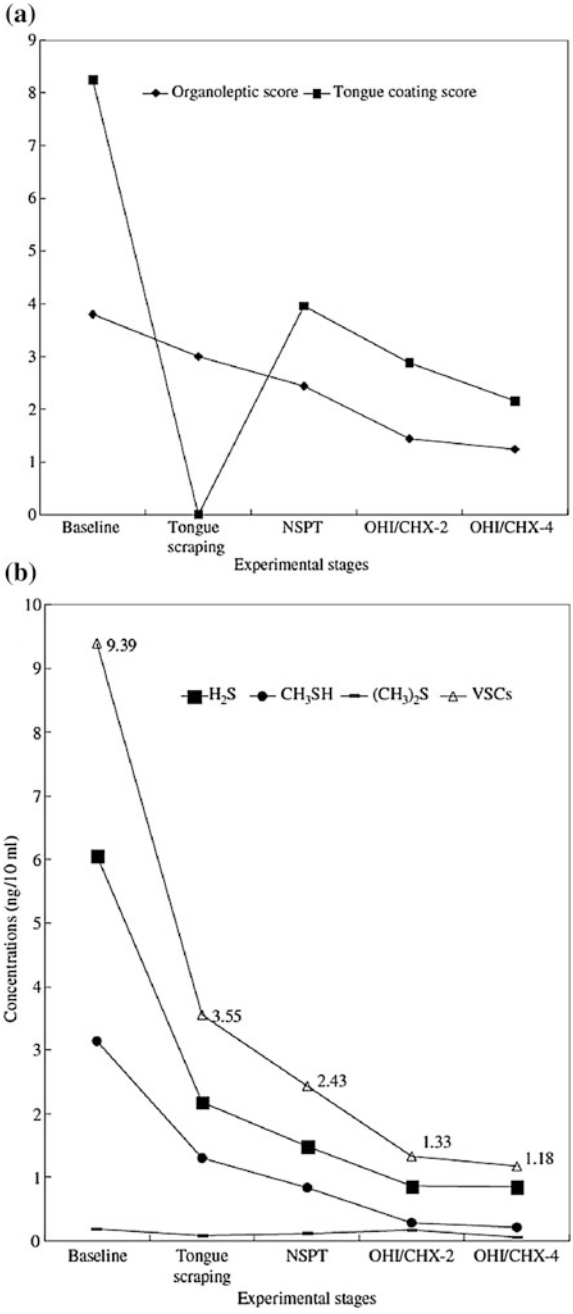

Fig. 1 **a** Changes on the organoleptic and tongue-coating scores. Data are expressed as the mean ± standard deviation from 25 subjects. Both scores were decreased by different treatments and were stage-dependent. **b** The VSCs concentrations of subjects at different experimental stages. Data are expressed as the mean ± standard deviation from 25 subjects. The concentrations of sulfur compounds were changed by different treatments and were dependent on the treatment stages. Reprinted with permission from Ref. [22]. Copyright (2008), Wiley

Table 3 Recent publications on chemiresistive SMO-based exhaled breath sensors for diagnosis of halitosis by detection of H_2S

Materials	Response definition	Sensitivity (response)	Detection limit	Testing ambient	Response/recovery time	Operating temp. (°C)	Ref.
Au-SnO_2 hollow sphere	R_{air}/R_{gas}	17.4 at 5 ppm	100 ppb	90 % RH	18 s/25 s	400	[32]
CuO-SnO_2 nanowire	R_{air}/R_{gas}	809 at 20 ppm	-/-	-/-	1–2 s/332 s	300	[33]
Mo-ZnO nanowire	R_{air}/R_{gas}	14.11 at 5 ppm	0.2 ppb	-/-	-/-	300	[34]
Pt-WO_3 nanofibers	R_{air}/R_{gas}	166.8 at 5 ppm	0.3 ppm	75 % RH	-/-	350	[35]
IrO_2-WO_3 nanofibers	R_{air}/R_{gas}	7.55 at 5 ppm	0.3 ppm	75 % RH	-/-	350	[35]
RGO-SnO_2 nanofiber	R_{air}/R_{gas}	34 at 5 ppm	1 ppm	95 % RH	198 s/114 s	200	[36]
Graphite-WO_3 hemitube	R_{air}/R_{gas}	19.66 at 5 ppm	100 ppb	90 % RH	8.4–11.6 s/12 s	300	[37]
WO_3 hemitube	R_{air}/R_{gas}	6.76 at 2 ppm	0.12 ppm	85 % RH	300 s /300 s	350	[38]
Three-dimensional WO_3 nanowire	R_{air}/R_{gas}	100 at 5 ppm	50 ppb	30 % RH	-/-	250	[39]

were heat-treated at 500 °C for 1 h to decompose the BCP spheres and crystallize the SnO_2 layer simultaneously with transfer of the Au nanoparticles onto the SnO_2 layer (Fig. 2c, d). SEM and TEM images of the Au-SnO_2 hollow sphere composite showed Au catalyst loading on the inner shell of the hollow SnO_2 spheres (white arrows) (Fig. 2e, g). To investigate the sensing characteristics of the Au-SnO_2 hollow spheres as well as pristine SnO_2 hollow spheres for exhaled breath sensing, they were tested at 400 °C in various gas analytes in a concentration range of 1–5 ppm at 90 % RH humidity. The result revealed improved H_2S sensing characteristics of Au-SnO_2 hollow spheres (R_{air}/R_{gas} = 17.4 at 5 ppm), with an almost threefold higher H_2S response relative to that (R_{air}/R_{gas} = 5.1 at 5 ppm) of the pristine SnO_2 hollow spheres. In particular, the Au-SnO_2 hollow spheres indicated a superior response toward 1 ppm of H_2S (R_{air}/R_{gas} = 7.3 at 1 ppm) in comparison with pristine SnO_2 hollow spheres (R_{air}/R_{gas} = 1.3 at 1 ppm) (Fig. 2h). In addition, selective detection capability was evaluated, revealing that a superior H_2S sensitive property was achieved using the Au-SnO_2 hollow spheres with minor responses (R_{air}/R_{gas} < 2.5 at 5 ppm) toward interfering gases such as C_5H_{12}, NO, NH_3, CO, C_7H_8, C_2H_5OH, and C_3H_6O (Fig. 2i). Au-SnO_2 hollow spheres could detect 100 ppb of H_2S with a high response (R_{air}/R_{air} = 5.7).

Stability is one of the most important parameters for reliable analysis of VSCs in exhaled breath using SMO-based sensors. Lee et al. [42] investigated long-term stability using ZnO, SnO_2, and WO_3 by cyclic exposure to hydrogen sulfide at 300 °C in highly humid ambient (80 % RH). It was concluded that ZnO and SnO_2 may not be suitable for exhaled breathe sensors due to sulfur contamination during hydrogen sulfide exposure, which results in unstable recovery. On the other hand, stable and reliable sensing characteristics were observed with WO_3, exhibiting a consistent response and recovery during cyclic exposure of hydrogen sulfide. This is attributed to the slight contamination of WO_3 to sulfur.

Thus far, a number of promising candidates have been proposed for real-time diagnosis of breath halitosis using diverse nanostructured catalyst-SMO composites. Several issues such as stability, selectivity, and reliability to detect VSCs must be addressed for commercialization as portable halitosis diagnostic devices.

2.2 Diabetes

Diabetes mellitus (DM) is a disease containing complex metabolic disorders caused by elevated blood glucose level, which can result in serious medical complications such as kidney failure, heart disease, blindness, limb amputation, and premature death [43]. There are two types of DM, i.e., type 1 diabetes mellitus (T1DM) for insulin-dependent and type 2 diabetes mellitus (T2DM) for non-insulin-dependent. T1DM is usually caused by an auto-immune reaction in which the body's defense system attacks the β cells that produce insulin. In the case of T2DM, insulin resistance and relative insulin deficiency are the major reasons for the disease. T1DM patients account for 15 % of the total DM patients, whereas the remaining

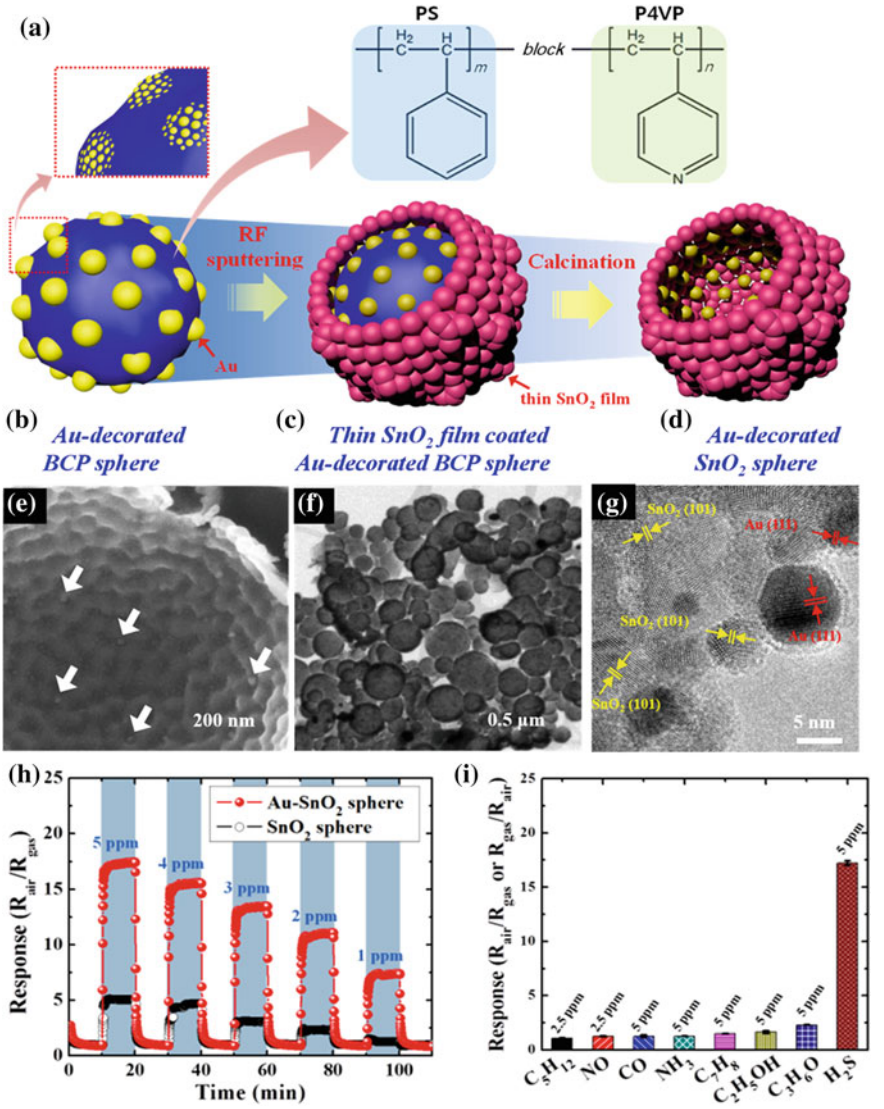

Fig. 2 **a** The chemical structure of the polystyrene-*b*-poly(4-vinylpyridine) (PS-*b*-P4VP) block copolymer, **b** Au decorated block copolymer with magnified schematic image (*red dotted box*), **c** thin SnO_2 film coated Au-decorated block copolymer sphere, and **d** Au-decorated SnO_2 (Au-SnO_2) hollow sphere after calcination at 500 °C for 1 h. **e** SEM image of the Au-SnO_2 spheres, **f** TEM image of the Au-SnO_2 hollow spheres, **g** high-resolution TEM (HRTEM) image of Au-SnO_2 hollow spheres, **h** H_2S gas sensing characteristics of Au-SnO_2 hollow spheres and pristine SnO_2 hollow spheres under 90 % RH ambient at 400 °C, **i** selective sensing characteristics of Au-SnO_2 hollow spheres toward H_2S in comparison with the interfering gases. Reprinted with permission from Ref. [32]. Copyright (2014), The Royal Society of Chemistry

85 % are T2DM patients. Recently, the International Diabetes Federation (IDF) reported that diabetes will be the 7th leading cause of death in 2030 and that the number of diabetes patients will remarkably increase by more than 50 % worldwide by 2030 compared to the number in 2011.

Typically, blood glucose levels are measured by pricking a finger for a drop of blood. This is not only a burden for DM patients but also can cause infection considering multiple daily checking for glucose monitoring. Considering the current diagnostic methods, it is a major advantage that diabetes can be simply identified by analyzing the concentration levels of biomarker (acetone) gases in exhaled breath, and glucose monitoring can be carried out in the same manner. For this reason, exhaled breath analysis for the diagnosis of diabetes and identifying the correlation between blood glucose levels and biomarker concentration have been intensively studied [44]. Generally, GC-MS are widely used for precise detect biomarker concentration in exhaled breath as well as in human plasma [45, 46].

Breath acetone has a strong correlation with T1DM, where elevated mean acetone concentration was observed in exhaled breath. Furthermore, other biomarkers for T1DM such as ethanol, methyl nitrate, xylene, and ethylbenzene have been identified [47, 48]. The basic mechanism of acetone generation in exhaled breath of diabetes patients is decarboxylation of acetoacetate, which derives from lipolysis or lipid peroxidation. The acetoacetate produces β-hydroxybutyrate, which can be used as an energy source in the body, and acetone, which can be exhaled from the lungs [49]. In previous studies, it was demonstrated that acetone concentration over 1.8 ppm was observed in diabetes patients; this is a 2–6 times higher concentration compared to that (300–900 ppb) of healthy subjects [50, 51]. However, such a strong correlation of exhaled acetone concentration with T2DM is still debated [44]. Recently, Yan et al. [52] successfully discriminated between T2DM patients (n = 48) and healthy people (n = 39), using GC-MS and identified additional biomarker gases, i.e., isopropanol and 2,3,4-trimethylhexane, for T2DM diagnosis. Greiter et al. [53] also demonstrated the possibility of discrimination between T2DM patients (n = 21) and healthy people (n = 26) by analyzing exhaled VOC profiles, using PTR-MS, where a distinct increase of acetone concentration was seen in T2DM patients.

Although the diagnosis of DM by exhaled breath analysis is promising, daily monitoring of blood glucose levels remains challenging. Recent studies demonstrated a high correlation between exhaled breath biomarkers and blood glucose level [43, 47, 54–57]. Lee et al. [47] investigated plasma glucose levels with 10 healthy young adults (5 men/5 women, mean 26 ± 4 year, range 21–33), using exhaled breath components such as acetone, ethanol, methyl nitrate, ethylbenzene, and xylene following the infusion of an intravenous glucose bolus. The experiment started with infusion of glucose and the transition of plasma glucose was monitored for 2 h. The plasma glucose level was elevated to 275.0 ± 9.8 mg/dl (range 231–317 mg/dl) after 2.5 min of glucose infusion and gradually lowered to 84.5 ± 1.8 mg/dl (range 74–94 mg/dl), which was slightly lower than that of the initial (fasting) plasma glucose, 94.5 ± 2.4 mg/dl (range 82–109 mg/dl). To estimate the plasma glucose level, four- (R4), five- (R5), and six-gas models (R6) were

established using exhaled acetone, ethanol, methyl nitrate, ethylbenzene, m/p-xylene, and o-xylene. The analyzed gas profiles exhibited strong correlations with the correlation coefficients (R4, R5, and R6) of 0.946 (range 0.701–0.993), 0.931 (range 0.699–0.991), and 0.913 (range 0.698–0.977). Figure 3a shows the plasma glucose profiles measured and estimated via exhaled breath components in the whole group of 10 subjects, which exhibited a strong correlation between plasma glucose and exhaled breath components. Turner et al. [43] performed an exhaled acetone analysis with respect to an insulin clamp with eight subjects of T1DM (mean 28 ± 3 years). The study was performed by the insulin clamp technique, i.e., a hypoglycemic clamp, in which the blood glucose level is stabilized during stepwise lowering from 5 to 2.4 mM for 40 min and subsequently exhaled breath was collected in each step. The insulin clamp technique presents two major advantages: accurate control over the blood glucose level of subjects with gradual change and acquisition of reliable exhaled acetone concentrations independent of variations of insulin in plasma. The collected exhaled breath was injected to SIFT-MS for a quantitative and real-time analysis of acetone and compared with the glucose level. The results revealed that there was a linear correlation between plasma glucose and exhaled breath acetone with all 8 subjects, where the exhaled breath acetone increased with the blood glucose (Fig. 3b). The opposite trend of the exhaled breath acetone concentration with respect to blood glucose level compared to results reported by several studies [55, 56, 58] is due to a number of conflicting metabolic signals of the body, which are attributed to the experimental procedure under hyperinsulinemic hypoglycemic conditions.

For commercial use as a portable diagnostic device with real-time monitoring, a highly sensitive diagnostic system that can be miniaturized and is based on simple measurement should be developed. Recently, chemiresistive-type SMOs have been garnering a great deal of attention for exhaled sensing layers in portable and real-time diabetes diagnostic applications. Table 4 lists recent publications on diabetes diagnosis by detection of acetone using SMO-based resistive-type sensing layers. Nanostructured SMOs using diverse materials have been intensively studied for highly sensitive detection of specific gas molecules [59–63]. In addition, noble metallic catalysts such as Pt, [35, 38] Pd, [64] and Au [65] as well as graphene-based catalytic materials such as graphite (GR), graphene oxide (GO), and reduced graphene oxide (RGO) have been integrated with nanostructured SMOs for selective acetone detection [36, 37, 66].

Righettoni et al. [55, 67–70] performed in-depth studies on the detection of acetone in exhaled breath using Si-doped WO_3 nanoparticles for the diagnosis of physical conditions including diabetes. Si-doped WO_3 nanoparticles as well as pure WO_3 nanoparticles were prepared by a flame spray pyrolysis on an Al_2O_3 substrate followed by *in situ* annealing for mechanical stabilization. Figure 4a, b show SEM and TEM images of the obtained pure WO_3 nanoparticles having average grain size of 13 nm. On the other hand, Si-doped WO_3 nanoparticles exhibited slightly decreased grain size of 10–12 nm, which was attributed to the formation of amorphous SiO_2 domains inhibiting the growth of WO_3 grain boundaries (Fig. 4c). The effects of sensing characteristics of Si-doped WO_3 nanoparticles depending on

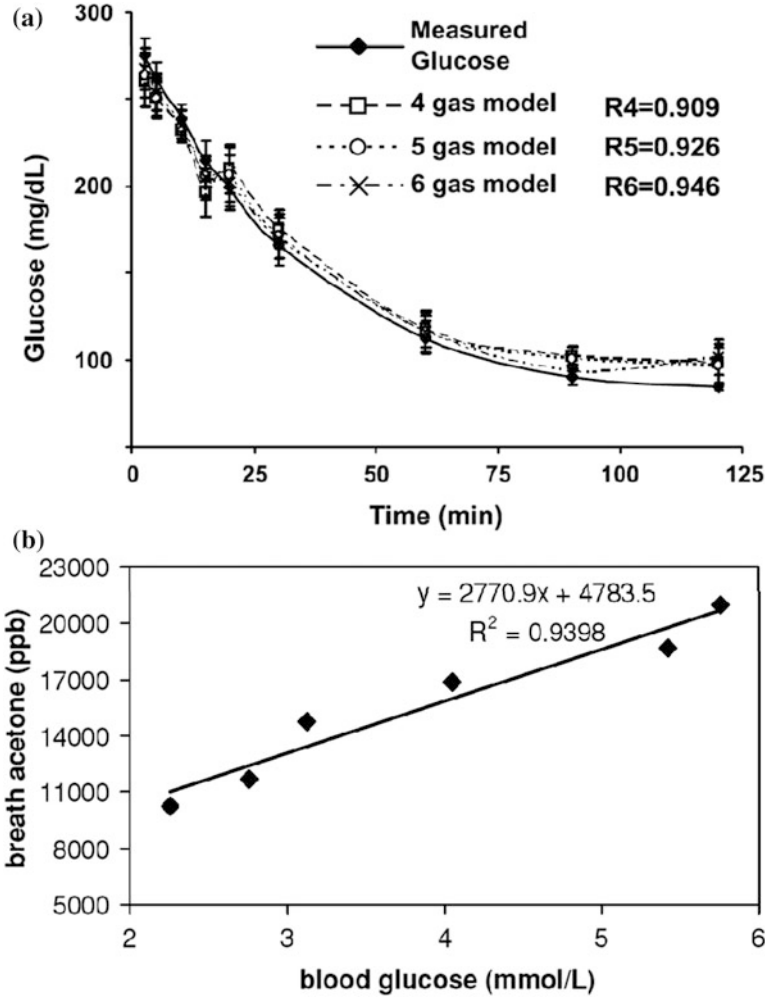

Fig. 3 **a** Plasma glucose profile directly measured from plasma serum and estimated via exhaled breath components such as acetone, ethanol, methyl nitrate, ethylbenzene, m/p-xylene, and o-xylene in the group of 10 subjects. R4, R5, and R6 are Pearson's correlation coefficients obtained by 4-, 5-, and 6-gas models, respectively. Reprinted with permission from Ref. [47]. Copyright (2009), The American Physiological Society. **b** Correlation between blood glucose and breath acetone concentrations of a T1DM subject having the strongest correlation. Reprinted with permission from Ref. [43]. Copyright (2009), IOP Publishing Ltd.

the Si-doping content under different humidity levels were investigated with respect to 600 ppb acetone at 400 °C (Fig. 4d). The results revealed that 10 mol% Si-doped WO_3 nanoparticles exhibited optimal acetone sensing characteristics with the highest acetone response ($R_{air}/R_{gas} - 1$) being 4.6 in dry air ambient. In addition, potential application for diagnosis of diabetes using 10 mol% Si-doped WO_3

Table 4 Recent publications on chemiresistive SMO-based exhaled breath sensors for potential diagnosis of diabetes by detection of acetone

Materials	Response definition	Sensitivity (response)	Detection limit	Testing ambient (% RH)	Response/recovery time	Operating temp. (°C)	Ref.
Pt-WO_3 NFs	R_{air}/R_{gas}	3.12 at 1 ppm	1 ppm	85	-/-	350	[35]
RGO-SnO_2 nanofiber	R_{air}/R_{gas}	10 at 5 ppm	1 ppm	95	<65 s/<25 s	350	[36]
Graphite-WO_3 hemitube	R_{air}/R_{gas}	6.96 at 5 ppm	100 ppb	90	<15 s/<30 s	300	[37]
Pt-WO_3 hemitube	R_{air}/R_{gas}	4.11 at 2 ppm	120 ppb	85	300 s/300 s	300	[38]
Pd-ZnO nanosheet	R_{air}/R_{gas}	~222 at 500 ppm	10 ppm	25	9 s/6 s	340	[64]
Au/α-Fe_2O_3	R_{air}/R_{gas}	5.91 at 1 ppm	1 ppm	45	0.5 s/20 s	270	[65]
Si-doped WO_3	$R_{air}/R_{gas} - 1$	1.5 at 0.6 ppm	20 ppb	90	78 s/74 s	400	[68]
C-doped WO_3	R_{air}/R_{gas}	3 at 1.8 ppm	200 ppb	95	3 − 9 s/6 − 12 s	300	[71]
Pt-SnO_2 nanofiber	$R_{air}/R_{gas} - 1$	2.5 at 2 ppm	120 ppb	80	15 s/-	400	[72]
WO_3 nanocrystal	R_{air}/R_{gas}	~4.5 at 5 ppm	50 ppb	65	30 s/30 s	300	[73]

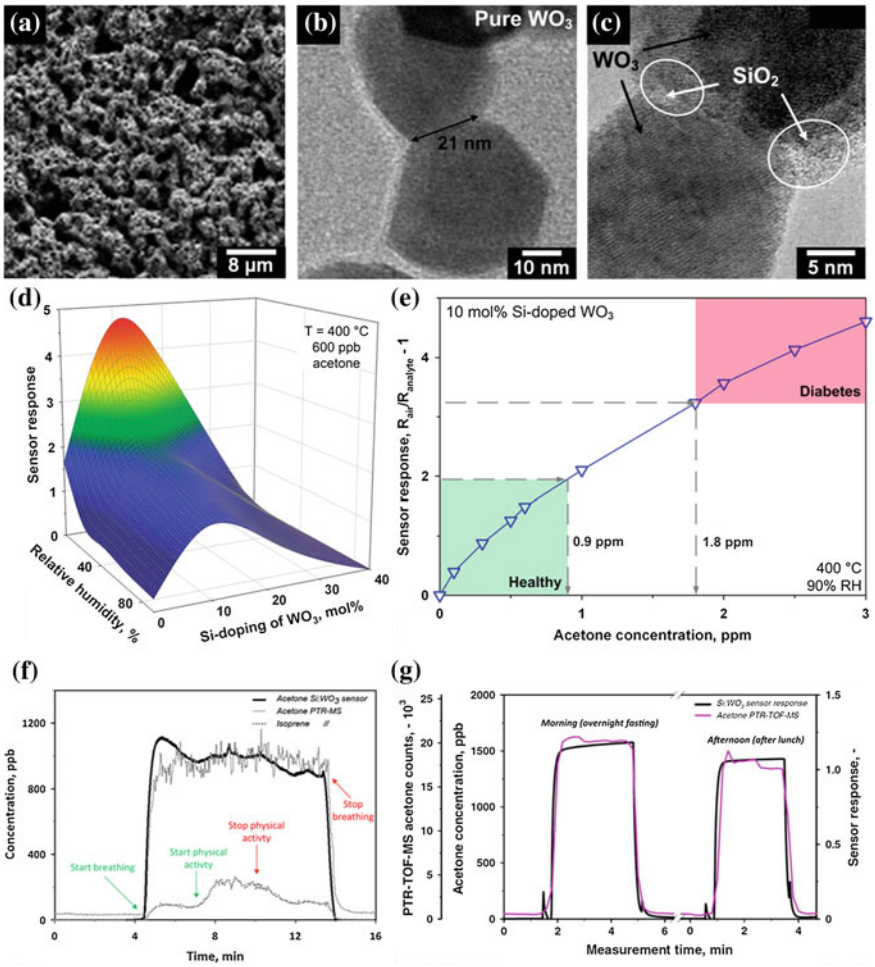

Fig. 4 **a** SEM image of pure WO_3 nanoparticles after in situ annealing. Reprinted with permission from Ref. [67]. Copyright (2011), IOP Publishing Ltd. TEM image of **b** pure WO_3 nanoparticles and **c** 20 mol% Si-doped WO_3 nanoparticles after annealing at 600 °C for 5 h in air. Reprinted with permission from Ref. [69]. Copyright (2010), American Chemical Society. **d** Acetone response characteristics of WO_3-based sensor with respect to the Si doping content and different relative humidity levels toward 600 ppb acetone at 400 °C. **e** Acetone response characteristics of 10 mol% Si-doped WO_3 nanoparticles in a concentration range of 0–3 ppm with 90 % RH at 400 °C. Reprinted with permission from Ref. [68]. Copyright (2010), American Chemical Society. **f** Exhaled acetone concentration measured by Si-doped WO_3 sensor (*thick solid line*) and acetone (*thin solid line*) and isoprene (*dotted line*) concentrations measured by PTR-MS during physical activity. Reprinted with permission from Ref. [70]. Copyright (2012), Elservier. **g** Comparison of exhaled breath acetone after overnight fasting and after lunch measured by Si-doped WO_3 sensor and PTR-TOF-MS. Reprinted with permission from Ref. [55]. Copyright (2013), IOP Publishing Ltd.

nanoparticles was demonstrated by measuring the acetone response in a concentration range of 0–3 ppm at 90 % RH. The results revealed a 40 % difference in sensor response between the concentration range of healthy people (<0.9 ppm) and the concentration range of diabetes patients (>1.8 ppm).

Real-time breath acetone monitoring as well as correlations between blood glucose and breath components were demonstrated using a portable Si-doped WO_3 sensor. The exhaled acetone concentration was evaluated by 10 mol% Si-doped WO_3 nanoparticles and compared with the acetone concentration measured by highly precise PTR-MS. As shown in Fig. 4f, 10 mol% Si-doped WO_3 nanoparticles exhibited reliable response characteristics with the calibrated acetone concentration of 970 ppb, which was in good agreement with the acetone concentration (980 ppb) measured by PTR-MS. In addition, 10 mol% Si-doped WO_3 nanoparticles showed a stable acetone sensing property regardless of physical activity, with the isoprene concentration showing a slight increase (100–240 ppb) [74]. Moreover, a correlation between blood glucose and exhaled acetone was demonstrated by measuring acetone concentration in the morning (overnight fasting) and afternoon (after lunch), using 10 mol% Si-doped WO_3 nanoparticles as well as proton transfer reaction time-of-flight mass spectrometry (PTR-TOF-MS). The breath acetone concentration decreased from 1600 to 1400 ppb after lunch (Fig. 4g), thus showing strong potential for application in real-time blood glucose monitoring by exhaled acetone analysis.

Recently, SMOs functionalized with graphene-based materials were proposed as an emerging exhaled breath sensing layers. Choi et al. proposed one dimensional (1D) structures of SMOs functionalized with graphene-based materials such as graphite (GR) and reduced graphene oxide (RGO) for application in potential diabetes diagnosis by detection of acetone (Fig. 5) [36, 37]. For example, 1D SnO_2 nanofibers were prepared by electrospinning and mixed with GO followed by a thermal reduction process at 500 °C in forming gas (20 % H_2/N_2) ambient to form RGO [36]. SEM and TEM images of an RGO-SnO_2 nanofiber composite showed flexible RGO nanosheets (white arrows) containing multiple SnO_2 nanofibers (Fig. 5a, b). Acetonesensing characteristics were investigated using pristine SnO_2 nanofibers as well as RGO-SnO_2 nanofiber composites having different RGO content (0.01 and 5 wt%) (Fig. 5c). Improved acetonesensing characteristics were revealed with observation of a 2.4-fold increased response (R_{air}/R_{gas} = 10.4 at 5 ppm) with 5 wt% RGO-loaded SnO_2 nanofibers compared to that (R_{air}/R_{gas} = 4.4 at 5 ppm) of pristine SnO_2 nanofibers at 350 °C. In addition, a highly porous 1D WO_3 hemitube structure was proposed and integrated into GR and GO for acetone sensing layers [37]. WO_3 hemitubes were synthesized by an electrospinning-assisted templating route [75] accompanied by physical vapor deposition, i.e., RF sputtering of a WO_3 thin layer on as-spun polymeric fibers. For a further increase of surface area, oxygen plasma treatment was performed to induce a rugged surface morphology of WO_3 hemitubes. GR and GO were then homogeneously mixed with WO_3 hemitubes to form GR- and GO-WO_3 hemitube composites. Folded and stacked graphene layers (white arrows) were observed in the GR-WO_3 hemitube composites (Fig. 5d). On the other hand, due to the flexible characteristic of GO

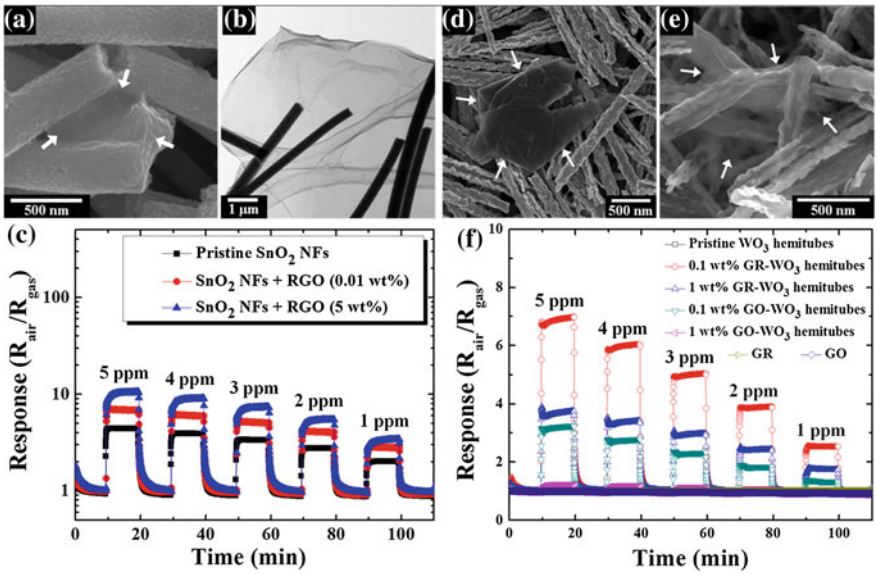

Fig. 5 **a** SEM and **b** TEM images of RGO-SnO_2 nanofiber composite. **c** Dynamic response transition of pristine SnO_2 nanofibers and RGO-SnO_2 nanofiber composite sensors in the acetone concentration range of 1–5 ppm at 350 °C. Reprinted with permission from Ref. [36]. Copyright (2014), American Chemical Society. SEM images of **d** GR and **e** GO-WO_3 hemitube composites, **f** dynamic response transition of pristine WO_3 hemitubes, GR-, and GO-WO_3 hemitube composite sensors in the acetone concentration range of 1–5 ppm at 300 °C. Reprinted with permission from Ref. [37]. Copyright (2014), American Chemical Society

(white arrows), it covered several WO_3 hemitubes (Fig. 5e). Acetone sensing characteristics of GR- and GO-WO_3 hemitube composites were evaluated in a concentration range of 1–5 ppm at 300 °C in highly humid atmosphere (85–95 % RH). The results revealed improved acetone sensing characteristics of 0.1 wt% GR-loaded WO_3 hemitubes (R_{air}/R_{gas} = 6.96 at 5 ppm) and 0.1 wt% GO-loaded WO_3 hemitubes (R_{air}/R_{gas} = 3.25 at 5 ppm) constituting 6.45-fold and threefold higher responses compared to that (R_{air}/R_{gas} = 1.08 at 5 ppm) of pristine WO_3 hemitubes. Single phases of GR and GO showed minor responses to acetone, which demonstrated that GR and GO act as catalysts when functionalized with WO_3 hemitubes. The improved acetone sensing characteristics of 1D SMOs functionalized with graphene-based materials were attributed to effective electronic sensitization of the graphene-based materials by forming Schottky barriers at the junction between SMO and the graphene-based materials, thereby modulating space charged layers when acetone was exposed. In addition to the enhanced response values, fast response (<15 s), a low limit of detection down to 100 ppb, and acetone selective sensing properties were demonstrated as well using 1D SMO nanostructures functionalized with graphene-based material composites, which showed high potential for real-time and portable devices for diagnosis of diabetes.

There will be many more opportunities to develop acetone sensitive and selective sensing layers by combining of SMOs functionalized with different catalysts for noninvasive diagnosis of diabetes as well as blood glucose monitoring by breath analysis.

2.3 *Fat Burning*

The amount of fat burning can be identified by analyzing exhaled breath [76]. It was reported that an increase in the concentration of exhaled acetone was found in those who control their diet to burn fat cells [74]. The increased acetone concentration is mainly due to the condition of ketosis, which results from burning fat cells to obtain energy for the body when the body does not have enough energy from carbohydrates. Based on this metabolism, it is possible to determine the daily diet conditions by the amount of fat burning. A fat burning indicator is particularly important considering the possible diagnosis of physical conditions. Fat burning is closely related to causes of fatigue, headaches, and nausea, which are caused by excessive fat burning.

A number of studies have demonstrated a correlation between fat burning and breath acetone concentration. Samudrala et al. [77] reported that monitoring of hepatic ketogenesis during walking can be achieved by measuring breath acetone concentration. The experiment proceeded with 23 nondiabetic subjects as well as 11 T1DM and 17 T2DM patients, analyzing breath acetone concentration using proton-transfer-reaction ion trap mass spectrometry (PIT-MS) before and after a 30–50 km walk on 4 consecutive days. Blood samples of each subject were collected to identify the correlation between breath acetone and hepatic ketogenesis. Distinctive changes were observed in breath acetone concentration before and after the walk measured over 4 consecutive days (Fig. 6a). Increased breath acetone concentration was observed in all subjects after the walk. In addition, repeated rising in breath acetone concentration in each consecutive day was presented, which implies that there was no significant effect of time. Breath acetone levels were compared with the groups of nondiabetic subjects (CT), T1DM, and T2DM before and after the walk on day 1 (Fig. 6b). Interestingly, significantly increased breath acetone concentration was observed with T1DM as well as moderate increase in CT subjects. However, a minor difference in breath acetone levels was observed before and after the walk with T2DM, suggesting lesser stimulation of ketogenesis in T2DM patients. The results revealed that breath acetone can provide real-time information of fat burning for daily lifestyle monitoring.

Recently, a portable breath acetone analyzer was developed for the daily monitoring of fat burning [78, 79]. The portable breath acetone analyzer developed by Toyooka et al. [78] was composed of two types of SMO-based sensors, i.e., Pt-doped WO_3 (tungsten oxide) and SnO_2 (tine oxide) (Fig. 6c). The sensing performance of the two sensors was evaluated by resistivity changes when the sensors were exposed to analytes at 400 °C. Pt-doped WO_3 was sensitive to acetone

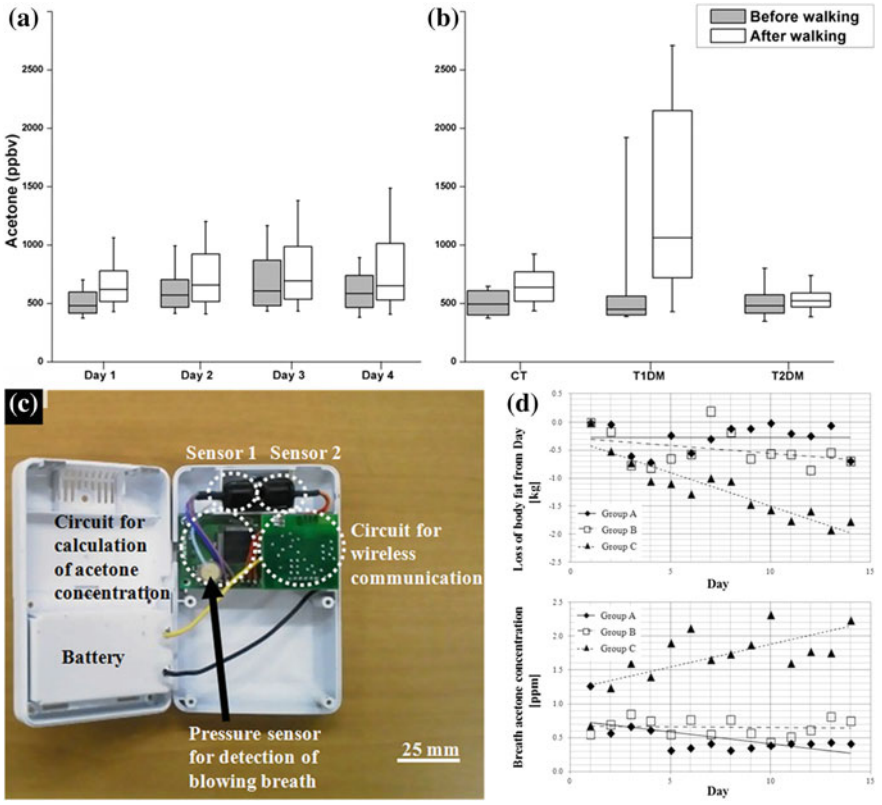

Fig. 6 **a** Monitoring of breath acetone concentration before and after the walk over 4 consecutive days with all subjects, **b** breath acetone concentration before and after the walk on the first day with each group of nondiabetic subjects (CT), T1DM, and T2DM. Reprinted with permission from Ref. [77]. Copyright (2014), Wiley. **c** Photograph of the portable breath acetone analyzer with the inside components, **d** average body fat loss (*upper*) and average breath acetone concentration (*lower*) of each group during 14 days. Reprinted with permission from Ref. [78]. Copyright (2013), IOP Publishing Ltd.

gas while SnO_2 was sensitive to a broad range of interfering gases such as hydrogen, ethylene, ethanol, and butylacetate, thereby accurately estimating acetone concentration with the effects of interfering gases. To investigate the breath acetone concentration depending on the physical conditions, all 17 subjects (11 men and 6 women) were divided into three groups, i.e., without controlled caloric intake or light exercise for group A, with light exercise such as jogging or fast walking for 30–60 min per day throughout the experiments for group B, and with controlled caloric intakes and light exercise for group C. Loss of body fat was monitored throughout the experiments from day 1 over 14 days and corresponding breath acetone was measured everyday using a portable analyzer (Fig. 6d). It was found that subjects in group A and group B exhibited no significant loss of fat and their breath acetone concentration was remained constant during 14 days. On the other

hand, the subjects who underwent enforced controlled caloric intake and light exercise in group C exhibited significant fat loss and their breath acetone approximately increased over 14 days. The results revealed that controlled caloric intake at the same time with light exercise stimulates fat loss, generating increased breath acetone concentration. In addition to breath acetone for the biomarker of fat burning, several components were identified as fat burning indicators from exhaled breath. King et al. [80] investigated exhaled VOCs under exercise conditions using PTR-MS and GC-MS. Particularly increased isoprene and methyl acetate concentrations were observed in exhaled breath shortly after the onset of exercise (e.g., approximately 1 min of pedaling).

The analysis of breath acetone is expected to receive more attention for monitoring of physical conditions such as fat burning because acetone is a blood-borne substance, which contains useful information of metabolism in the body. Several types of breath acetone analyzers in the form of portable prototypes are being developed for daily lifestyle monitoring, and present a promising outlook for realizing a noninvasive and simple analysis method.

2.4 Lung Cancer

Lung cancer is the most common cancer worldwide and a fatal disease showing a high mortality rate. It is important to diagnose lung cancer in the early stage because it determines life expectancy. If lung cancer is diagnosed in stage I, the 5-year survival rate is 58–73 %, but the rate drops dramatically to 3.5 % for those diagnosed in a later stage [81]. Conventionally, lung cancer was detected by computed tomography (CT) or bronchoscopy in hospital. However, CT showed low sensitivity and bronchoscopy is a costly and invasive diagnostic method, and accordingly is not a suitable screening method for large populations. Such disadvantages may result in late detection of lung cancer (only 15 % detection at a localized stage [82]) and high mortality rates.

As an alternative lung cancer screening method, exhaled breath analysis has been intensively researched for many years due to advantages such as noninvasiveness and a simple diagnostic method [83, 84]. A number of studies revealed that multiple VOCs are closely related to lung cancer, as summarized in Table 5. These VOCs produced or metabolized endogenously can provide useful information for lung cancer detection considering that the VOCs, which are exhaled from the lungs after traveling through the bloodstream, reflect metabolic properties of the body's tissues [85].

A number of VOCs related to lung cancer were identified with GC-MS. Song et al. [91] found the characteristic VOCs including 1-butanol and 3-hydroxy-2-butanone from the exhaled breath of patients with non-small-cell lung cancer (NSCLC) by examining 43 patients and comparing the results with 41 normal controls. However, it was also found that there is no significant difference in VOC levels with different stages of lung cancer patients [91]. In addition, Poli et al. [92]

Table 5 Identified VOCs for lung cancer detection

Disease	Identified VOCs for lung cancer detection	Ref.
Lung cancer	Butane; 3-methyl tridecane; 7-methyl tridecane; 4-methyl octane; 3-methyl hexane; heptane; 2-methyl hexane, pentane; 5-methyl decane	[86]
Lung cancer	Adenocarcinoma-2,4,6-trimethyloctane; 2-methyldodecane; 2-tridecanone; 2-pentadecanone; 8-methy lheptadecane; 2-heptadecanone; nonadecane; eicosane; squamous-methanoic acid; 2-nonanone; 2-pentadecanone; nonadecane; eicosane; SCC- 2-decanone; 2-hendecanone; 2-methylnaphthaline; 2-tridecanone; 2-pentadecanone; 2,6-dimethylnaphthaline; 1-heptadecanol; 2-heptadecanone; nonadecane; eicosane	[87]
Lung cancer	Aldehydes-butanal; formaldehyde; acetaldehyde; pentanal; hexanal; octanal; nonanal	[88]
Lung cancer	1-methyl-4-(1-methylethyl)benzene; toluene; dodecane; 3,3-dimethyl pentane; 2,3,4-trimethyl hexane; 1,10-(1-butenylidene)bis benzene	[89]
Lung cancer	isobutane; methanol; ethanol; acetone; pentane; isoprene; isopropanol; dimethylsulfide; carbon disulfide; benzene; toluene	[90]
Non-small cell lung cancer	1-butanol and 3-hydroxy-2-butanone	[91]
Lung cancer	2-methyl pentane; pentane; ethyl benzene; xylenes (total); trimethyl benzene; toluene; benzene; decane; octane; penta methyl heptane	[92]

identified and quantified 13 VOCs, including 6 alkanes and 6 aromatic hydrocarbons (e.g., 2-methylpentane; pentane, ethylbenzene, trimethylbenzene, heptane, and isoprene) using GC-MS for the early diagnosis of NSCLC. The experiment was carried out with 36 NSCLC patients and control subjects of 35 smokers and 50 nonsmokers. The results revealed that exhaled breath of nonsmoking controls exhibited higher levels of isoprene and heptane than that of NSCLC patients, whereas lower levels of almost all substances out of 13 VOCs were observed with nonsmoking controls compared to those of NSCLC patients and smoker controls. The analysis demonstrated the potential use of GC-MS as a complementary test together with conventional diagnostic methods for the early diagnosis of lung cancer with high specificity of 93.6 %.

Recently, several types of simple, relatively inexpensive, and portable exhaled breath analyzing devices such as ion mobility spectrometers, [93] a quartz microbalance, [94, 95] a colorimetric sensor array, [96–98] and electronic nose [90, 99] have been developed and demonstrated the potential for diagnosis of lung cancer. Among the various sensing techniques, chemiresistive-type sensors are receiving much attention due to high portability and a simple operating principle. Peng et al. [100] synthesized monolayer-capped Au nanoparticles as a VOCs sensing layer for the diagnosis of lung cancer by comparing the exhaled breath between 56 healthy subjects with nonsmokers and 40 patients with primary stage III and stage IV lung cancer. Au nanoparticles, which have an average diameter of 5 nm, were

synthesized to have 9 different organic functionalities (dodecanethiol, decanethiol, 1-butanethiol, 2-ethylhexanethiol, hexanethiol, tert-dodecanethiol, 4-methoxy-toluenethiol, 2-mercaptobenzoxazole and 11-mercapto-1-undecanol) and sensor arrays were composed using Au decorated with organic functionalities. The collected exhaled breath from the healthy subjects and lung cancer patients was injected into the sensor array for 5 min in vacuum ambient and the sensor signals were collected. There were distinctive differences in response signals, $\Delta R/R_b$, (where R_b is the baseline resistance of the sensor in the absence of an analyte and ΔR is the baseline-corrected steady-state resistance change upon exposure of the sensor to analyte) of 11-mercapto-1-undecanol-gold nanoparticles (red circles) and decanethiol-gold nanoparticles (black squares) between the healthy subjects (filled symbols) and the lung cancer patients (open symbols) showing a positive response (Fig. 7a). In addition, the variation of the sensor response using 2-mercaptobenzoxazole-gold nanoparticles (red diamonds) and tert-dodecanethiol-gold nanoparticles (black triangles) was observed, exhibiting negative response characteristics toward exhaled breath from healthy subjects (filled symbols) and the lung cancer patients (open symbols) (Fig. 7b). The results revealed that clear discrimination between the health subject and the lung cancer subject was possible by injecting exhaled breath to the sensors without a preconcentration or dehumidification process. The measured data were analyzed by using a standard principle component analysis (PCA), which is a statistical method to effectively reduce the multidimensional data space to its main components for visualization of the differentiation ability of the sensor array [101]. Figure 7c shows well-defined clusters for healthy states and lung cancer states using real human breath as well as simulated breath composed of artificial VOCs mixtures, [102] which demonstrated the capability of lung cancer diagnosis in a fast, reliable, and noninvasive manner. In addition, Barash et al. [103] demonstrated a unique odor print of NSCLC with 18 molecularly modified gold nanoparticles. The analysis was performed by measuring headspace emitted from the lung cancer cells and control medium. Distinctive differences were observed from the typical response curves of 2-mercaptobenzoxazole-gold nanoparticles (circles) and 2-mercaptobenzoxazole-gold nanoparticles with 1 % carbon black (squares) toward the headspace of NOSCLC (filled symbols) and control medium (empty symbols) exhibiting a positive response (Fig. 7d). In addition, decanethiol-gold nanoparticles (rhombuses) exhibited a negative response transition when exposed to the headspace of NOSCLC (filled symbols) and control medium (empty symbols) (Fig. 7e). The higher responses of the sensors toward NSCLC compared to that of the control medium was attributed to generation of the detected VOCs from cancer cells [104]. On the other hand, it can be interpreted that in the case of sensors exhibiting higher responses toward the control medium, the detected VOCs are consumed by the cancer cells [105]. All 18-sensor arrays were analyzed by PCA, as shown in Fig. 7f. The PCA diagram shows well-defined clusters without overlap for the NSCLC and the control patterns. These features imply that clear discrimination is possible using Au nanoparticle-based sensors without a time-consuming preconcentration step of the analyte.

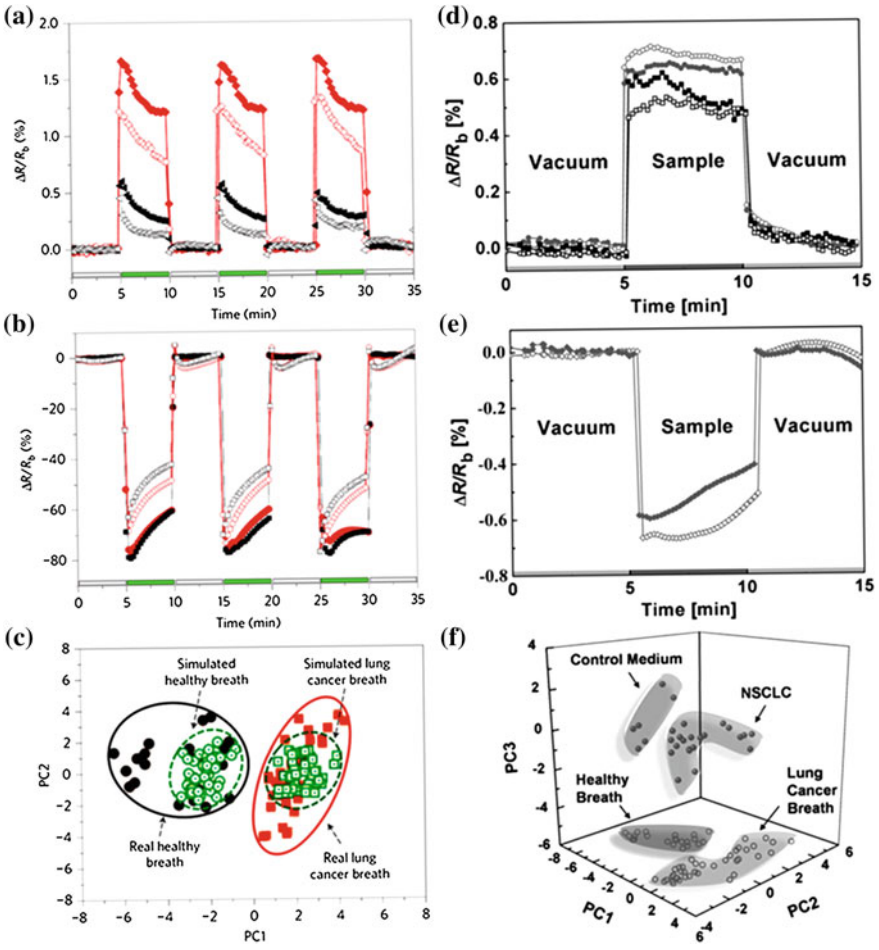

Fig. 7 **a** Typical response ($\Delta R/R_b$) characteristics of 11-mercapto-1-undecanol-gold nanoparticles (*red circles*) and decanethiol-gold nanoparticles (*black squares*) toward exhaled breath of healthy subject (*filled symbols*) and lung cancer patients (*open symbols*), **b** Typical response ($\Delta R/R_b$) characteristics of 2-mercaptobenzoxazole-gold nanoparticles (*red diamonds*) and tert-dodecanethiol-gold nanoparticles (*black triangles*) toward exhaled breath of healthy subject (*filled symbols*) and lung cancer patients (*open symbols*), and **c** PCA using real human breath and simulated breath. Reprinted with permission from Ref. [100]. Copyright (2009), Nature Publishing Group. **d** Typical response ($\Delta R/R_b$) characteristics of 2-mercaptobenzoxazole-gold nanoparticles (*circles*), 2-mercaptobenzoxazole-gold nanoparticles with 1 % carbon black (*squares*), and **e** decanethiol-gold nanoparticles (*rhombuses*) toward the headspace of NOSCLC (*filled symbols*) and control medium (*empty symbols*), and **f** PCA of the multidimensional $\Delta R/R_b$ data set of NSCLC and control medium. Reprinted with permission from Ref. [103]. Copyright (2009), Wiley

Recently, SMO-based sensing layers were developed for the potential diagnosis of lung cancer. Kim et al. [106] proposed a highly sensitive and selective exhaled breath sensor using Pd-loaded WO_3 nanofiber for the detection of toluene gas in exhaled breath. WO_3 nanofibers were prepared by electrospinning, which is a facile and versatile route to obtain a nonwoven web structure. The nanofibers can facilitate effective gas diffusion and also offer enhanced surface reaction. Pd catalysts were embedded within the WO_3 nanofibers, which was achieved by dissolving a Pd precursor during the electrospinning process and subsequent heat treatment. In addition, Pd nanoparticles (6–10 nm), synthesized by a polyol process, were decorated on the surface of WO_3 nanofibers. Thus, Pd catalysts were sensitized at both the inside and outside of WO_3 nanofibers. The structural and morphological observations revealed a highly porous 1D structure of WO_3 nanofibers as well as functionalization of Pd nanoparticles (Fig. 8a). Toluene sensing characteristics were

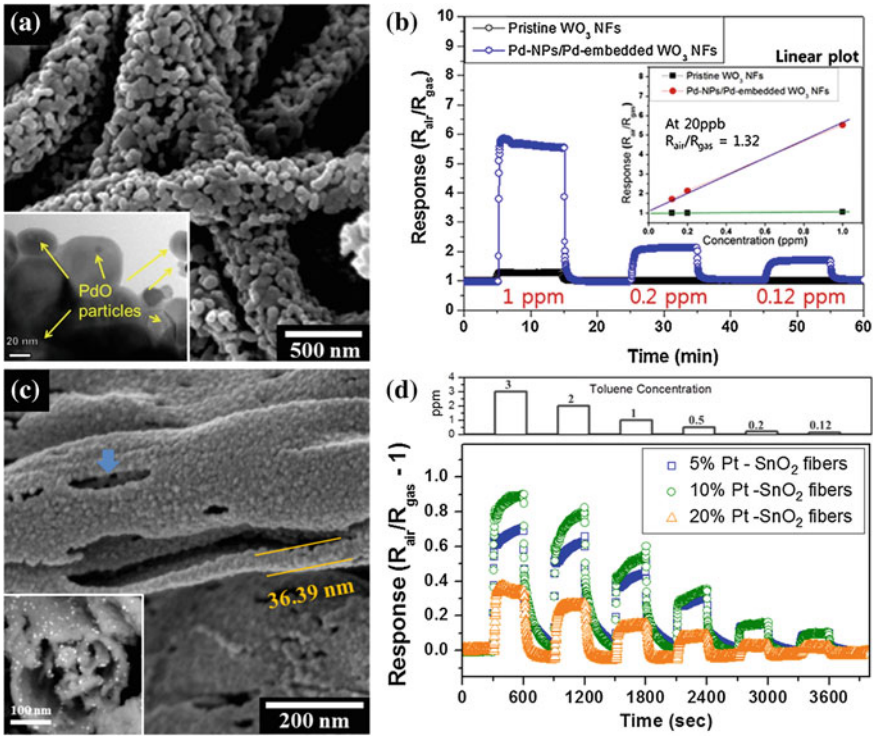

Fig. 8 **a** SEM image of Pd-NPs/Pd-embedded WO_3 nanofibers with TEM image in the inset, and **b** dynamic response transition toward cyclic toluene exposure at 350 °C with linear response approximation in the *inset*. Reprinted with permission from Ref. [106]. Copyright (2014), Elservier. **c** SEM image of thin-walled SnO_2 nanofibers. Inset image shows Pt functionalized thin-walled SnO_2 nanofibers, and **d** dynamic response transition toward cyclic toluene exposure with different Pt loading on the SnO_2 nanofibers at 300 °C. Reprinted with permission from Ref. [72]. Copyright (2013), Wiley

evaluated at 350 °C in a highly humid atmosphere (90 % RH) to demonstrate potential application in lung cancer diagnosis. A fourfold improved toluene sensing response (R_{air}/R_{gas} = 5.5 at 1 ppm) was achieved using Pd nanoparticle/Pd-embedded WO_3 nanofibers compared to that (R_{air}/R_{gas} = 1.27 at 1 ppm) of pristine WO_3 nanofibers without Pd functionalization (Fig. 8b). In addition, toluene selective properties were achieved, exhibiting a minor response toward interfering analytes such as acetone and hydrogen sulfide. The limit of the detection property was investigated by linear approximation, which predicted a toluene response of 1.32 at 20 ppb (Fig. 8b inset).

Shin et al. [72] also demonstrated potential application of thin-walled SnO_2 nanofibers functionalized with Pt nanoparticles for the diagnosis of lung cancer based on the detection of toluene in exhaled breath. Thin-walled SnO_2 nanofibers exhibited elongated pores with a broad size distribution along the fiber direction, which can facilitate gas penetration of large size VOCs through the pores (Fig. 8c). Highly porous thin-walled SnO_2 nanofibers were obtained by controlling the electrospinning parameter, i.e., flow rate, to induce effective phase separation between polymer domains (polyvinyl acetate matrix polymer) and Sn precursor (Sn (IV) acetate) domains. In addition, Pt nanoparticles, which were synthesized by a polyol process, were functionalized with the thin-walled SnO_2 nanofibers to optimize the toluene sensing characteristics (Fig. 8c inset). The cyclic toluene response characteristic was investigated in a concentration range of 120 ppb to 3 ppm at 300 °C (Fig. 8d). The results revealed that 10 % Pt functionalized thin-wall SnO_2 nanofibers exhibited a dramatically improved toluene sensing response ($R_{air}/R_{gas}-1$ = 0.9 at 3 ppm) compared to that ($R_{air}/R_{gas}-1 < 0.1$ at 3 ppm) of pristine SnO_2 nanofibers. In addition, stable toluene response and recovery characteristics were observed with 10 % Pt functionalized thin-wall SnO_2 nanofibers down to 120 ppb with a response of 0.1.

Even though there have been several promising results for the potential diagnosis of lung cancer using chemiresistive-type sensors based on SMO sensing layers, there are several issues to be addressed such as sensitivity, selectivity, stability, and reliability in relation to VOCs. In addition, clinical studies with large numbers of subjects should be accompanied for clinical application.

3 Summary and Future Perspective

Clinical demonstrations identifying correlations between concentrations of biomarkers in exhaled breath and specific diseases have been introduced using several types of breath analyzing techniques such as GC/MS, SIFT-MS, and PTR-MS as well as chemiresistive-type gas sensors. Exhaled breath analysis is a very important screening method because it is a noninvasive and simple diagnostic method. Potential suitability in early diagnosis for T1DM has been suggested through the monitoring of exhaled breath acetone concentration. In addition, promising results for the diagnosis of T2DM were also reported. Even though significant efforts have

been exerted to find a correlation between the blood glucose level and breath acetone biomarkers, further in-depth clinical study should be performed on a large population of subjects for daily blood glucose monitoring using exhaled breath analysis.

In the case of lung cancer detection, highly precise breath analyzing techniques should be developed for clinical application in conjunction with conventional diagnostic approaches such as CT and bronchoscopy, thereby increasing screening capability in the early stage and reducing the mortality rate. In addition to the diagnostic application, portable or wearable daily healthcare devices using breath analysis, which can monitor oral halitosis and fat burning, can be developed for better quality of life.

Several emerging analysis methods and the development of accurate detection techniques for biomarker components provide a bright perspective for diagnosis of different diseases using exhaled breath analysis. In particular, electronic noses, which are composed of cross-sensitive sensor arrays with pattern recognition algorithms, present several advantages compared to other types of analyzing equipment with respect to portability and cost effectiveness for hand-held breath analysis devices.

Acknowledgement This work is supported by the Center for Integrated Smart Sensors funded by the Ministry of Science, ICT & Future Planning as the Global Frontier Project.

References

1. Tisch U, Haick H (2014) Chemical sensors for breath gas analysis: the latest developments at the breath analysis summit 2013. J Breath Res 8(2):027103
2. Arasaradnam RP, Covington JA, Harmston C, Nwokolo CU (2014) Review article: next generation diagnostic modalities in gastroenterology-gas phase volatile compound biomarker detection. Aliment Pharm Ther 39(8):780–789
3. Eckel SP, Baumbach J, Hauschild AC (2014) On the importance of statistics in breath analysis-hope or curse? J Breath Res 8(1):012001
4. Kim KH, Jahan SA, Kabir E (2012) A review of breath analysis for diagnosis of human health. Trac-Trend Anal Chem 33:1–8
5. Di Natale C, Paolesse R, Martinelli E, Capuano R (2014) Solid-state gas sensors for breath analysis: a review. Anal Chim Acta 824:1–17
6. Mazzatenta A, Di Giulio C, Pokorski M (2013) Pathologies currently identified by exhaled biomarkers. Resp Physiol Neurobi 187(1):128–134
7. Broza YY, Haick H (2013) Nanomaterial-based sensors for detection of disease by volatile organic compounds. Nanomedicine 8(5):785–806
8. Buszewski B, Kesy M, Ligor T, Amann A (2007) Human exhaled air analytics: biomarkers of diseases. Biomed Chromatogr 21(6):553–566
9. Pijnenburg MW, Floor SE, Hop WC, De Jongste JC (2006) Daily ambulatory exhaled nitric oxide measurements in asthma. Pediatr Allergy Immu 17(3):189–193
10. Selby A, Clayton B, Grundy J, Pike K, Drew K, Raza A, Kurukulaaratchy R, Arshad SH, Roberts G (2010) Are exhaled nitric oxide measurements using the portable NIOX MINO repeatable? Resp Res 11(43):1–9

11. Phillips M, Gleeson K, Hughes JMB, Greenberg J, Cataneo RN, Baker L, McVay WP (1999) Volatile organic compounds in breath as markers of lung cancer: a cross-sectional study. Lancet 353(9168):1930–1933
12. Oneill HJ, Gordon SM, Oneill MH, Gibbons RD, Szidon JP (1988) A computerized classification technique for screening for the presence of breath biomarkers in lung-cancer. Clin Chem 34(8):1613–1618
13. Cheng WH, Lee WJ (1999) Technology development in breath microanalysis for clinical diagnosis. J Lab Clin Med 133(3):218–228
14. Prince BJ, Milligan DB, McEwan MJ (2010) Application of selected ion flow tube mass spectrometry to real-time atmospheric monitoring. Rapid Commun Mass Sp 24 (12):1763–1769
15. Dummer JF, Storer MK, Hu WP, Swanney MP, Milne GJ, Frampton CM, Scotter JM, Prisk GK, Epton MJ (2010) Accurate, reproducible measurement of acetone concentration in breath using selected ion flow tube-mass spectrometry. J Breath Res 4(4):046001
16. Ajibola OA, Smith D, Spanel P, Ferns GA (2013) Effects of dietary nutrients on volatile breath metabolites. J Nutr Sci 2:e34
17. Lindinger W, Hansel A, Jordan A (1998) Proton-transfer-reaction mass spectrometry (PTR-MS): on-line monitoring of volatile organic compounds at pptv levels. Chem Soc Rev 27(5):347–354
18. Kim ID, Rothschild A (2011) Nanostructured metal oxide gas sensors prepared by electrospinning. Polym Advan Technol 22(3):318–325
19. Tangerman A, Winkel EG (2010) Extra-oral halitosis: an overview. J Breath Res 4 (1):017003
20. Whittle CL, Fakharzadeh S, Eades J, Preti G (2007) Human breath odors and their use in diagnosis. Ann Ny Acad Sci 1098:252–266
21. Ciaffoni L, Peverall R, Ritchie GAD (2011) Laser spectroscopy on volatile sulfur compounds: possibilities for breath analysis. J Breath Res 5(2):024002
22. Tsai CC, Chou HH, Wu TL, Yang YH, Ho KY, Wu YM, Ho YP (2008) The levels of volatile sulfur compounds in mouth air from patients with chronic periodontitis. J Periodontal Res 43(2):186–193
23. Scully C, Greenman J (2008) Halitosis (breath odor). Periodontol 2000 48:66–75
24. Porter SR, Scully C (2006) Oral malodour (halitosis). Brit Med J 333(7569):632–635
25. Kazor CE, Mitchell PM, Lee AM, Stokes LN, Loesche WJ, Dewhirst FE, Paster BJ (2003) Diversity of bacterial Populations on the tongue dorsa of patients with halitosis and healthy patients. J Clin Microbiol 41(2):558–563
26. Hughes FJ, McNab R (2008) Oral malodour-a review. Arch Oral Biol 53:S1–S7
27. Kim JG, Kim YJ, Yoo SH, Lee SJ, Chung JW, Kim MH, Park DK, Hahm KB (2010) Halimeter ppb levels as the predictor of erosive gastroesophageal reflux disease. Gut Liver 4 (3):320–325
28. Tanda N, Washio J, Ikawa K, Suzuki K, Koseki T, Iwakura M (2007) A new portable sulfide monitor with a zinc-oxide semiconductor sensor for daily use and field study. J Dent 35 (7):552–557
29. Tangerman A, Winkel EG (2008) The portable gas chromatograph OralChroma (TM): a method of choice to detect oral and extra-oral halitosis. J Breath Res 2(1):017010
30. Kim ID, Rothschild A, Tuller HL (2013) Advances and new directions in gas-sensing devices. Acta Mater 61(3):974–1000
31. Jang BH, Landau O, Choi SJ, Shin J, Rothschild A, Kim ID (2013) Selectivity enhancement of SnO_2 nanofiber gas sensors by functionalization with Pt nanocatalysts and manipulation of the operation temperature. Sens Actuators B 188:156–168
32. Choi SJ, Kim MP, Lee SJ, Kim BJ, Kim ID (2014) Facile Au catalyst loading on the inner shell of hollow SnO_2 spheres using Au-decorated block copolymer sphere templates and their selective H_2S sensing characteristics. Nanoscale 6(20):11898–11903

33. Dong KY, Choi JK, Hwang IS, Lee JW, Kang BH, Ham DJ, Lee JH, Ju BK (2011) Enhanced H_2S sensing characteristics of Pt doped SnO_2 nanofibers sensors with micro heater. Sens Actuators, B 157(1):154–161
34. Woo HS, Kwak CH, Kim ID, Lee JH (2014) Selective, sensitive, and reversible detection of H_2S using Mo-doped ZnO nanowire network sensors. J Mater Chem A 2(18):6412–6418
35. Shin J, Choi SJ, Youn DY, Kim ID (2012) Exhaled VOCs sensing properties of WO_3 nanofibers functionalized by Pt and IrO_2 nanoparticles for diagnosis of diabetes and halitosis. J Electroceram 29(2):106–116
36. Choi SJ, Jang BH, Lee SJ, Min BK, Rothschild A, Kim ID (2014) Selective detection of acetone and hydrogen sulfide for the diagnosis of diabetes and halitosis using SnO_2 nanofibers functionalized with reduced graphene oxide nanosheets. ACS Appl Mater Interfaces 6(4):2587–2596
37. Choi SJ, Fuchs F, Demadrille R, Grevin B, Jang BH, Lee SJ, Lee JH, Tuller HL, Kim ID (2014) Fast responding exhaled-breath sensors using WO_3 hemitubes functionalized by graphene-based electronic sensitizers for diagnosis of diseases. ACS Appl Mater Interfaces 6 (12):9061–9070
38. Choi SJ, Lee I, Jang BH, Youn DY, Ryu WH, Park CO, Kim ID (2013) Selective diagnosis of diabetes using Pt-functionalized WO_3 hemitube networks as a sensing layer of acetone in exhaled breath. Anal Chem 85(3):1792–1796
39. Ponzoni A, Comini E, Sberveglieri G, Zhou J, Deng SZ, Xu NS, Ding Y, Wang ZL (2006) Ultrasensitive and highly selective gas sensors using three-dimensional tungsten oxide nanowire networks. Appl Phys Lett 88(20):203101
40. Kim MP, Ku KH, Kim HJ, Jang SG, Yi GR, Kim BJ (2013) Surface intaglio nanostructures on microspheres of gold-cored block copolymer spheres. Chem Mater 25(21):4416–4422
41. Kim MP, Kang DJ, Jung DW, Kannan AG, Kim KH, Ku KH, Jang SG, Chae WS, Yi GR, Kim BJ (2012) Gold-decorated block copolymer microspheres with controlled surface nanostructures. ACS Nano 6(3):2750–2757
42. Lee I, Choi SJ, Park KM, Lee SS, Choi S, Kim ID, Park CO (2014) The stability, sensitivity and response transients of ZnO, SnO_2 and WO_3 sensors under acetone, toluene and H_2S environments. Sens Actuators B 197:300–307
43. Turner C, Walton C, Hoashi S, Evans M (2009) Breath acetone concentration decreases with blood glucose concentration in type I diabetes mellitus patients during hypoglycaemic clamps. J Breath Res 3(4):046004
44. Wang ZN, Wang CJ (2013) Is breath acetone a biomarker of diabetes? A historical review on breath acetone measurements. J Breath Res 7(3):037109
45. Fan GT, Yang CL, Lin CH, Chen CC, Shih CH (2014) Applications of Hadamard transform-gas chromatography/mass spectrometry to the detection of acetone in healthy human and diabetes mellitus patient breath. Talanta 120:386–390
46. Deng CH, Zhang W, Zhang J, Zhang XM (2004) Rapid determination of acetone in human plasma by gas chromatography-mass spectrometry and solid-phase microextraction with on-fiber derivatization. J Chromatogr B 805(2):235–240
47. Lee J, Ngo J, Blake D, Meinardi S, Pontello AM, Newcomb R, Galassetti PR (2009) Improved predictive models for plasma glucose estimation from multi-linear regression analysis of exhaled volatile organic compounds. J Appl Physiol 107(1):155–160
48. Novak BJ, Blake DR, Meinardi S, Rowland FS, Pontello A, Cooper DM, Galassetti PR (2007) Exhaled methyl nitrate as a noninvasive marker of hyperglycemia in type 1 diabetes. P Natl Acad Sci USA 104(40):15613–15618
49. Miekisch W, Schubert JK, Noeldge-Schomburg GFE (2004) Diagnostic potential of breath analysis-focus on volatile organic compounds. Clin Chim Acta 347(1–2):25–39
50. Deng CH, Zhang J, Yu XF, Zhang W, Zhang XM (2004) Determination of acetone in human breath by gas chromatography-mass spectrometry and solid-phase microextraction with on-fiber derivatization. J Chromatogr B 810(2):269–275
51. Diskin AM, Spanel P, Smith D (2003) Time variation of ammonia, acetone, isoprene and ethanol in breath: a quantitative SIFT-MS study over 30 days. Physiol Meas 24(1):107–119

52. Yan YY, Wang QH, Li WW, Zhao ZJ, Yuan X, Huang YP, Duan YX (2014) Discovery of potential biomarkers in exhaled breath for diagnosis of type 2 diabetes mellitus based on GC-MS with metabolomics. RSC Adv 4(48):25430–25439
53. Greiter MB, Keck L, Siegmund T, Hoeschen C, Oeh U, Paretzke HG (2010) Differences in exhaled gas profiles between patients with type 2 diabetes and healthy controls. Diabetes Technol Ther 12(6):455–463
54. Hu W (2005) Breath ethanol and acetone as indicators of serum glucose levels: an initial report. Ethnic Dis 15(3):32–34
55. Righettoni M, Schmid A, Amann A, Pratsinis SE (2013) Correlations between blood glucose and breath components from portable gas sensors and PTR-TOF-MS. J Breath Res 7 (3):037110
56. Turner C, Parekh B, Walton C, Spanel P, Smith D, Evans M (2008) An exploratory comparative study of volatile compounds in exhaled breath and emitted by skin using selected ion flow tube mass spectrometry. Rapid Commun Mass Spectrom 22(4):526–532
57. Minh TDC, Oliver SR, Ngo J, Flores R, Midyett J, Meinardi S, Carlson MK, Rowland FS, Blake DR, Galassetti PR (2011) Noninvasive measurement of plasma glucose from exhaled breath in healthy and type 1 diabetic subjects. Am J Physiol-Endoc M 300(6):E1166–E1175
58. Smith D, Spanel P (1996) Application of ion chemistry and the SIFT technique to the quantitative analysis of trace gases in air and on breath. Int Rev Phys Chem 15(1):231–271
59. Cho NG, Woo HS, Lee JH, Kim ID (2011) Thin-walled NiO tubes functionalized with catalytic Pt for highly selective C_2H_5OH sensors using electrospun fibers as a sacrificial template. Chem Commun 47(40):11300–11302
60. Choi SH, Hwang IS, Lee JH, Oh SG, Kim ID (2011) Microstructural control and selective C_2H_5OH sensing properties of Zn_2SnO_4 nanofibers prepared by electrospinning. Chem Commun 47(33):9315–9317
61. Yang DJ, Kamienchick I, Youn DY, Rothschild A, Kim ID (2010) Ultrasensitive and highly selective gas sensors based on electrospun SnO_2 nanofibers modified by Pd Loading. Adv Funct Mater 20(24):4258–4264
62. Chang YE, Youn DY, Ankonina G, Yang DJ, Kim HG, Rothschild A, Kim ID (2009) Fabrication and gas sensing properties of hollow SnO_2 hemispheres. Chem Commun 27:4019–4021
63. Kim ID, Rothschild A, Lee BH, Kim DY, Jo SM, Tuller HL (2006) Ultrasensitive chemiresistors based on electrospun TiO_2 nanofibers. Nano Lett 6(9):2009–2013
64. Xiao YH, Lu LZ, Zhang AQ, Zhang YH, Sun L, Huo L, Li F (2012) Highly enhanced acetone sensing performances of porous and single crystalline ZnO nanosheets: high percentage of exposed (100) facets working together with surface modification with Pd nanoparticles. ACS Appl Mater Interfaces 4(8):3797–3804
65. Gunawan P, Mei L, Teo J, Ma JM, Highfield J, Li QH, Zhong ZY (2012) Ultrahigh sensitivity of Au/1D α-Fe_2O_3 to acetone and the sensing mechanism. Langmuir 28 (39):14090–14099
66. Choi S-J, Ryu W-H, Kim S-J, Cho H-J, Kim I-D (2014) Bi-functional co-sensitization of graphene oxide sheets and Ir nanoparticles on p-type Co_3O_4 nanofibers for selective acetone detection. J Mater Chem B 2(41):7160–7167
67. Righettoni M, Tricoli A (2011) Toward portable breath acetone analysis for diabetes detection. J Breath Res 5(3):1–16
68. Righettoni M, Tricoli A, Pratsinis SE (2010) Si: WO_3 sensors for highly selective detection of acetone for easy diagnosis of diabetes by breath analysis. Anal Chem 82(9):3581–3587
69. Righettoni M, Tricoli A, Pratsinis SE (2010) Thermally stable, silica-doped epsilon-WO_3 for sensing of acetone in the human breath. Chem Mater 22(10):3152–3157
70. Righettoni M, Tricoli A, Gass S, Schmid A, Amann A, Pratsinis SE (2012) Breath acetone monitoring by portable Si: WO_3 gas sensors. Anal Chim Acta 738:69–75
71. Xiao T, Wang XY, Zhao ZH, Li L, Zhang L, Yao HC, Wang JS, Li ZJ (2014) Highly sensitive and selective acetone sensor based on C-doped WO_3 for potential diagnosis of diabetes mellitus. Sens Actuators B 199:210–219

72. Shin J, Choi SJ, Lee I, Youn DY, Park CO, Lee JH, Tuller HL, Kim ID (2013) Thin-wall assembled SnO_2 fibers functionalized by catalytic Pt nanoparticles and their superior exhaled-breath-sensing properties for the diagnosis of diabetes. Adv Funct Mater 23 (19):2357–2367
73. Shi JC, Hu GJ, Sun Y, Geng M, Wu J, Liu YF, Ge MY, Tao JC, Cao M, Dai N (2011) WO_3 nanocrystals: synthesis and application in highly sensitive detection of acetone. Sens Actuators B 156(2):820–824
74. King J, Kupferthaler A, Unterkofler K, Koc H, Teschl S, Teschl G, Miekisch W, Schubert J, Hinterhuber H, Amann A (2009) Isoprene and acetone concentration profiles during exercise on an ergometer. J Breath Res 3(2):027006
75. Choi SH, Ankonina G, Youn DY, Oh SG, Hong JM, Rothschild A, Kim ID (2009) Hollow ZnO nanofibers fabricated using electrospun polymer templates and their electronic transport properties. ACS Nano 3(9):2623–2631
76. Kundu SK, Bruzek JA, Nair R, Judilla AM (1993) Breath acetone analyzer—diagnostic-tool to monitor dietary-fat loss. Clin Chem 39(1):87–92
77. Samudrala D, Lammers G, Mandon J, Blanchet L, Schreuder THA, Hopman MT, Harren FJM, Tappy L, Cristescu SM (2014) Breath acetone to monitor life style interventions in field conditions: an exploratory study. Obesity 22(4):980–983
78. Toyooka T, Hiyama S, Yamada Y (2013) A prototype portable breath acetone analyzer for monitoring fat loss. J Breath Res 7(3):036005
79. Landini BE, Bravard ST (2009) Breath acetone concentration measured using a palm-size enzymatic sensor system. IEEE Sens J 9(12):1802–1807
80. King J, Mochalski P, Kupferthaler A, Unterkofler K, Koc H, Filipiak W, Teschl S, Hinterhuber H, Amann A (2010) Dynamic profiles of volatile organic compounds in exhaled breath as determined by a coupled PTR-MS/GC-MS study. Physiol Meas 31(9):1169–1184
81. Taivans I, Bukovskis M, Strazda G, Jurka N (2014) Breath testing as a method for detecting lung cancer. Expert Rev Anticanc 14(2):121–123
82. American Cancer Society (2014) Cancer facts and figures 2014. American Cancer Society, Atlanta
83. Dent AG, Sutedja TG, Zimmerman PV (2013) Exhaled breath analysis for lung cancer. J Thorac Dis 5:S540–S550
84. Chan HP, Lewis C, Thomas PS (2009) Exhaled breath analysis: novel approach for early detection of lung cancer. Lung Cancer 63(2):164–168
85. Mazzone PJ (2012) Exhaled breath volatile organic compound biomarkers in lung cancer. J Breath Res 6(2):027106
86. Phillips M, Cataneo RN, Cummin ARC, Gagliardi AJ, Gleeson K, Greenberg J, Maxfield RA, Rom WN (2003) Detection of lung cancer with volatile markers in the breath. Chest 123(6):2115–2123
87. Wang YS, Hu YJ, Wang D, Yu K, Wang L, Zou YC, Zhao C, Zhang XL, Wang P, Ying KJ (2012) The analysis of volatile organic compounds biomarkers for lung cancer in exhaled breath, tissues and cell lines. Cancer Biomark 11(4):129–137
88. Fuchs P, Loeseken C, Schubert JK, Miekisch W (2010) Breath gas aldehydes as biomarkers of lung cancer. Int J Cancer 126(11):2663–2670
89. Peng G, Hakim M, Broza YY, Billan S, Abdah-Bortnyak R, Kuten A, Tisch U, Haick H (2010) Detection of lung, breast, colorectal, and prostate cancers from exhaled breath using a single array of nanosensors. Brit J Cancer 103(4):542–551
90. Machado RF, Laskowski D, Deffenderfer O, Burch T, Zheng S, Mazzone PJ, Mekhail T, Jennings C, Stoller JK, Pyle J, Duncan J, Dweik RA, Erzurum SC (2005) Detection of lung cancer by sensor array analyses of exhaled breath. Am J Resp Crit Care 171(11):1286–1291
91. Song G, Qin T, Liu H, Xu GB, Pan YY, Xiong FX, Gu KS, Sun GP, Chen ZD (2010) Quantitative breath analysis of volatile organic compounds of lung cancer patients. Lung Cancer 67(2):227–231

92. Poli D, Carbognani P, Corradi M, Goldoni M, Acampa O, Balbi B, Bianchi L, Rusca M, Mutti A (2005) Exhaled volatile organic compounds in patients with non-small cell lung cancer: cross sectional and nested short-term follow-up study. Resp Res 6(71):1–10
93. Westhoff M, Litterst P, Freitag L, Urfer W, Bader S, Baumbach JI (2009) Ion mobility spectrometry for the detection of volatile organic compounds in exhaled breath of patients with lung cancer: results of a pilot study. Thorax 64(9):744–748
94. Di Natale C, Macagnano A, Martinelli E, Paolesse R, D'Arcangelo G, Roscioni C, Finazzi-Agro A, D'Amico A (2003) Lung cancer identification by the analysis of breath by means of an array of non-selective gas sensors. Biosens Bioelectron 18(10):1209–1218
95. D'Amico A, Pennazza G, Santonico M, Martinelli E, Roscioni C, Galluccio G, Paolesse R, Di Natale C (2010) An investigation on electronic nose diagnosis of lung cancer. Lung Cancer 68(2):170–176
96. Mazzone PJ, Hammel J, Dweik R, Na J, Czich C, Laskowski D, Mekhail T (2007) Diagnosis of lung cancer by the analysis of exhaled breath with a colorimetric sensor array. Thorax 62 (7):565–568
97. Huo DQ, Xu YH, Hou CJ, Yang M, Fa HB (2014) A novel optical chemical sensor based AuNR-MTPP and dyes for lung cancer biomarkers in exhaled breath identification. Sens Actuators B 199:446–456
98. Ono K, Sugio K, Uramoto H, Baba T, Ichiki Y, Takenoyama M, Hanagiri T, Oyama T, Yasumoto K (2009) Discrimination of multiple primary lung cancers from intrapulmonary metastasis based on the expression of four cancer-related proteins. Cancer 115(15):3489–3500
99. Dragonieri S, Annema JT, Schot R, van der Schee MPC, Spanevello A, Carratu P, Resta O, Rabe KF, Sterk PJ (2009) An electronic nose in the discrimination of patients with non-small cell lung cancer and COPD. Lung Cancer 64(2):166–170
100. Peng G, Tisch U, Adams O, Hakim M, Shehada N, Broza YY, Billan S, Abdah-Bortnyak R, Kuten A, Haick H (2009) Diagnosing lung cancer in exhaled breath using gold nanoparticles. Nat Nanotechnol 4(10):669–673
101. Rock F, Barsan N, Weimar U (2008) Electronic nose: current status and future trends. Chem Rev 108(2):705–725
102. Peng G, Trock E, Haick H (2008) Detecting simulated patterns of lung cancer biomarkers by random network of single-walled carbon nanotubes coated with nonpolymeric organic materials. Nano Lett 8(11):3631–3635
103. Barash O, Peled N, Hirsch FR, Haick H (2009) Sniffing the unique "odor print" of non-small-cell lung cancer with gold nanoparticles. Small 5(22):2618–2624
104. Filipiak W, Sponring A, Mikoviny T, Ager C, Schubert J, Miekisch W, Amann A, Troppmair J (2008) Release of volatile organic compounds (VOCs) from the lung cancer cell line CALU-1 in vitro. Cancer Cell Int 8(17):1–11
105. Joseph Y, Guse B, Vossmeyer T, Yasuda A (2008) Gold nanoparticle/organic networks as chemiresistor coatings: the effect of film morphology on vapor sensitivity. J Phys Chem C 112(32):12507–12514
106. Kim NH, Choi SJ, Yang DJ, Bae J, Park J, Kim ID (2014) Highly sensitive and selective hydrogen sulfide and toluene sensors using Pd functionalized WO_3 nanofibers for potential diagnosis of halitosis and lung cancer. Sens Actuators B 193:574–581

http://www.springer.com/978-94-017-9980-5

Smart Sensors for Health and Environment Monitoring

Kyung, C.-M. (Ed.)
2015, VI, 323 p. 166 illus., 121 illus. in color., Hardcover
ISBN: 978-94-017-9980-5